Article

The Inhibition of Oxidative Stress-Mediated Cell Apoptosis by the Caspase Inhibitor (S)-3-((S)-2-(6-(2,3-dihydrobenzo[b][1,4]dioxin-6-yl)-1-oxoisoindolin-2-yl)butanamido)-4-oxo-5-(2,3,5,6-tetrafluorophenoxy)pentanoic Acid in Human Dermal Papilla Cells

Bomi Park [1], Daeun Kim [1], Yurim Lee [2], Seihyun Choi [2], HeeDong Park [2], Sanghwa Lee [2] and Jaesung Hwang [1,*]

[1] Department of Genetic & Biotechnology, Graduate School of Biotechnology, College of Life Sciences, Kyung Hee University, Youngin 17104, Republic of Korea; pbm1208@khu.ac.kr (B.P.); kpkdy0107@khu.ac.kr (D.K.)

[2] Innovo Therapeutics Inc., 507 38, Mapo-daero, Mapo-gu, Seoul 04174, Republic of Korea; yrlee@innovothera.com (Y.L.); seihyun@innovothera.com (S.C.); hdpark@innovothera.com (H.P.); shlee@innovothera.com (S.L.)

* Correspondence: jshwang@khu.ac.kr

Abstract: Alopecia is traditionally viewed as androgen-dependent, but emerging evidence has implicated oxidative stress in the pathogenesis of hair loss. Current treatments for alopecia have limited efficacy, leading to the need for new therapies. Human dermal papilla cells (hDPCs) play a pivotal role in hair follicle (HF) development and hair growth regulation. In this study, we investigated the potential of (S)-3-((S)-2-(6-(2,3-dihydrobenzo[b][1,4]dioxin-6-yl)-1-oxoisoindolin-2-yl)butanamido)-4-oxo-5-(2,3,5,6 tetrafluorophenoxy) pentanoic acid (THPA), a pan-caspase inhibitor, to reduce ROS-induced cellular damage and apoptosis in hDPCs. Our study revealed that THPA effectively suppressed hydrogen peroxide-induced apoptosis while also attenuating activated caspase signaling. Additionally, THPA restored the down-regulated expression of β-catenin, a key mediator of the Wnt/β-catenin pathway, in hDPCs exposed to hydrogen peroxide. Furthermore, significant alterations in Akt/mTOR/p70S6K signaling were observed following THPA treatment. Notably, THPA treatment led to a reduction in the expression of Dickkopf-1 (DKK-1), an inhibitor of the Wnt/β-catenin pathway implicated in hair follicle regression. Moreover, THPA treatment decreased the expression of the cell senescence markers p21 and p16, suggesting a potential role in preserving hDPC function and delaying hair follicle regression. Collectively, our findings highlight the therapeutic potential of THPA in preventing hair loss by protecting hDPCs against oxidative stress damage.

Keywords: alopecia; apoptosis; caspase; reactive oxygen species; human dermal papilla cells; β-catenin; Akt; senescence

1. Introduction

Alopecia is a common form of hair loss affecting both men and women. Up to 80% of men and 50% of women are affected by alopecia, which becomes more common and severe as people age [1]. While alopecia may not directly damage the body, it can cause patients to experience severe psychological stress that can lead to negative feelings such as inferiority, anxiety, and despair and negatively impact their quality of life and personal social activities [2]. Consequently, it is critical to manage alopecia appropriately. Topical minoxidil and oral finasteride are two Food and Drug Administration-approved therapies. Minoxidil is known as a direct-acting arteriolar vasodilator that expands blood flow to induce growth in hair follicles, and finasteride is a 5-alpha reductase inhibitor that prevents testosterone from converting into dihydrotestosterone (DHT), thus affecting hair loss [3]. However, these medications can partially stop hair loss but do not fully

stimulate hair growth. Moreover, negative side effects and the challenge of adhering to daily treatment regimens may further limit their use [4,5]. Therefore, recent research has explored therapeutic approaches such as pharmaceuticals and nutritional supplements like vitamins and plant extracts, highlighting the essential need for new treatments to increase hair growth [6].

Hair follicles consist of keratinocytes and a specialized mesenchymal cell population known as dermal papilla cells (DPCs) [7,8]. Human dermal papilla cells (hDPCs) are pivotal in follicle development, regeneration, and hair growth cycling. hDPCs stimulate follicular keratinocytes to maintain and regenerate the hair follicle cycle [9]. By secreting growth-promoting signals, hDPCs play essential roles in regulating the onset of anagen and the transition from the anagen to catagen phases [10]. Recently, DPCs have been used in in vitro screening models to assess the efficacy of agents that target hair growth.

Alopecia is characterized as an age-related or androgen-dependent mechanism in hDPCs [11]. However, clinical reports have demonstrated that alopecia does not occur solely through androgen-dependent pathways; it also involves androgen-independent mechanisms, such as those induced by chemotherapy and stress [12–14]. Recent studies have shown that apoptotic and senescent levels are markedly elevated in balding DPCs compared to non-balding DPCs [15,16]. Interestingly, reactive oxygen species (ROS) have emerged as crucial inducers to both androgen-dependent and androgen-independent alopecia [12], with higher ROS levels detected in the dermal papilla of balding scalps than in non-balding scalps [17,18]. Elevated ROS levels correlate with reduced DPC motility [15] and heightened cell senescence in balding-scalp DPCs [15]. Recent studies have linked cisplatin-induced alopecia to ROS production and ROS-mediated apoptosis in DPCs [19]. These findings suggest that targeting ROS is a promising and necessary approach in the development of alopecia prevention and treatment strategies.

The Wnt/β-catenin signaling pathway plays a crucial role in the development of hair follicles [6,20,21]. Following activation in adult tissues, β-catenin, the primary mediator of the Wnt/β-catenin signaling pathway, aggregates within the cytoplasm before translocating to the nucleus. Within the nucleus, it forms complexes with transcription factors from the lymphoid enhancer factor/T-cell factor (Lef/Tcf) family [22]. This complex orchestrates the transcription of target genes that are crucial for regulating fundamental cellular functions such as proliferation and migration [23]. Also, exposure to H_2O_2 decreased the length of human hair follicles through the modulation of the GSK-3β/β-catenin signaling pathway [24].

Apoptosis, a highly regulated programmed cell death process, plays a pivotal role in various physiological and pathological conditions. It is essential for maintaining tissue homeostasis by eliminating damaged or unwanted cells. Considering the widespread use of H_2O_2 to induce oxidative stress-related apoptosis, we adopted an in vitro model to simulate oxidative stress using H_2O_2 [25,26]. Research has indicated that H_2O_2, along with superoxide and hydroxyl radicals, plays a role in damaging hDPCs, ultimately contributing to hair loss [24,27].

In this study, we developed a novel pan-caspase inhibitor, (S)-3-((S)-2-(6-(2,3-dihydrobenzo[b][1,4]dioxin-6-yl)-1-oxoisoindolin-2-yl)butanamido)-4-oxo-5-(2,3,5,6-tetrafluorophenoxy)pentanoic acid (THPA). We aimed to demonstrate that THPA could ameliorate hair loss by modulating cell apoptosis and regulating the associated signaling pathways. This was confirmed by inducing oxidative stress with H_2O_2 in hDPCs.

2. Materials and Methods

2.1. Synthetic Method of (S)-3-((S)-2-(6-(2,3-dihydrobenzo[b][1,4]dioxin-6-yl)-1-oxoisoindolin-2-yl)butanamido)-4-oxo-5-(2,3, 5,6-tetrafluorophenoxy)pentanoic Acid

(1)   Synthetic scheme of Compound **6**

To the solution of 4-Benzyl N-(tert-Butoxycarbonyl)-L-aspartate (25 g, 77.3 mmol) and N-methylmorpholine (9.35 mL, 85.0 mmol) in tetrahydrofuran (250 mL) under nitrogen

gas at −15 °C, we added isobutyl chloroformate (10.53 mL, 81.2 mmol) dropwise. After stirring at −15 °C for 30 min, the mixture was warmed to 0 °C.

Freshly prepared excess diazomethane (5.0 eq) in ether was added to the solution at 0 °C under nitrogen (until the yellowish color did not disappear). The reaction mixture was stirred at 0 °C for 30 min.

The reaction mixture was treated with 5 N HBr/glacial acetic acid (1:1) (30.9 mL, 2 eq, 154.6 mmol) slowly. After stirring at 0 °C for 30 min, the mixture was partitioned between ethyl acetate and water. The organic phase was washed successively with water, saturated sodium bicarbonate, and saturated sodium chloride. The solution was dried over anhydrous sodium sulfate, filtered and evaporated to dryness. Hexane was added and the solid was filtered and washed with hexane to provide Compound **4** (25 g, 80.8% over three steps).

To a solution of Compound **4** (25 g, 62.5 mmol) in DMF (250 mL), we added potassium fluoride (9.068 g, 156.3 mmol) and 2,3,5,6-tetrafluorophenol (11.408 g, 68.8 mmol). The reaction mixture was stirred at room temperature for 2 h and then partitioned between ethyl acetate and water. The organic layer was washed with sat. ammonium chloride and brine. The organic layer was dried over sodium sulfate, filtered, and concentrated. The crude product directly went to the next step.

Compound **5** was treated with 4 N HCl in dioxane (155 mL), and the reaction mixture was stirred at r. t. for 1 h. The solution was concentrated under reduced pressure. The remaining one was stirred in anhydrous diethyl ether for 1 h. The solid was filtered, washed with EtOAc, and dried to produce the desired Compound **6** (23.6 g, 90% over two steps) (Figure 1).
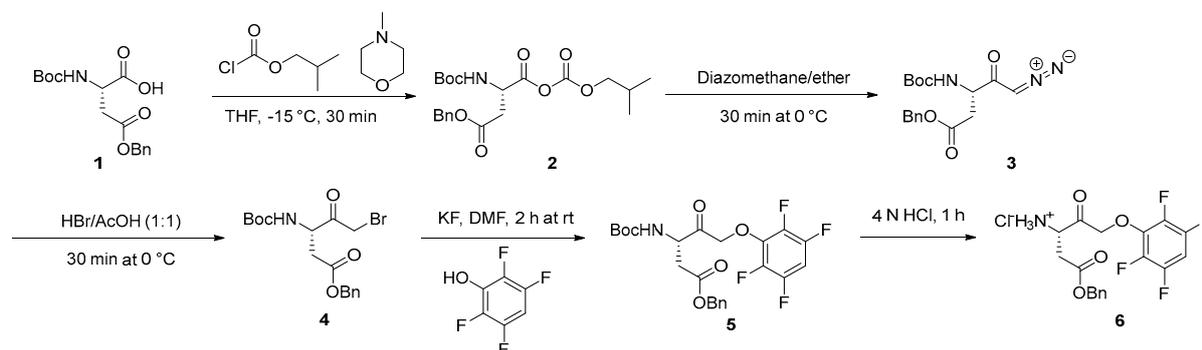
Figure 1. Synthetic scheme of Compound **6**.

(2)   Method used to make diazomethane

N-methylurea (86 g, 1.162 mol) was dissolved in water (715 mL). Sodium nitrite (88.2 g, 1.278 mol) was added, and the mixture was cooled to 0 °C in an ice bath. Then, 33% aq. hydrochloric acid (170 mL, 1.51 mol) was added dropwise over a period of 1 h. The mixture was left to stir for 30 min at the same temperature. The precipitate was filtered off, washed with water, and dried in vacuo. N-methyl-N-nitrosourea (74.8 g, 62%) was obtained as a light-beige powder (it was stored at −28 °C).

N-methyl-N-nitrosourea was introduced into an Erlenmeyer flask containing diethyl ether and 40% aq. KOH previously cooled to 0 °C in an ice bath. The mixture was left to stand for 30 min at 0 °C, carefully shaking it several times. The organic phase containing the generated diazomethane was decanted and dried (KOH pellets) at 0 °C for 3 h.

(3)   Synthetic scheme of (S)-3-((S)-2-(6-(2,3-dihydrobenzo[b][1,4]dioxin-6-yl)-1-oxoisoin-
        dolin-2-yl)butanamido)-4-oxo-5-(2,3,5,6-tetrafluorophenoxy)pentanoic acid

To the solution of Compound **7** (Methyl 5-Bromo-2-methylbenzoate) (25 g, 109.14 mmol) and N-bromosuccimide (19.424 g, 109.14 mmol) in CHCl3 (100 mL), we added dibenzoyl peroxide (1.322 g, 5.46 mmol). The reaction mixture was stirred at 75 °C for 1 h and then

diluted with dichloromethane and water. The organic layer was washed with water (three times) and brine, then dried with sodium sulfate and concentrated under reduced pressure to produce Compound 8.

To the solution of Compound **8** (from the previous reaction) and tert-butyl (2S)-2-aminobutanoate hydrochloride (21.287 g, 108.78 mmol) in acetonitrile (300 mL), we added diisopropylethyl amine (DIPEA) (56.84 mL, 326.33 mmol). The reaction mixture was stirred under reflux for 5 h. The solution was cooled to room temperature and then diluted with ethyl acetate. The solution was washed with water, saturated ammonium chloride, and brine; dried over sodium sulfate; and concentrated under reduced pressure. The crude product was purified by crystallization with ether and hexane to produce Compound **9** (25.1 g, 65%).

To the solution of Compound **9** (10.0 g, 28.32 mmol) in 1,4-dioxane (100 mL), we added Tetrakis(triphenylphosphine)palladium (3.26 g, 2.83 mmol), 2 M potassium carbonate solution (28.2 mL, 56.5 mmol) and 2,3-dihydro-1,4-benzodioxin-6-ylboronic acid (5.58 g, 29.73 mmol) The reaction mixture was degassed for 10 min. The reaction solution was refluxed at 100 °C for 10 h and cooled to room temperature. The solution was diluted with ethyl acetate and water and filtered through a Celite pad. The organic layer was washed with saturated ammonium chloride, brined, dried over sodium sulfate, and concentrated using a rotary evaporator. The crude product was used for the next step without any purification.

Compound **10** was treated with 4 N HCl in dioxane (20 eq, 142 mL), and the reaction mixture was stirred at room temperature for 8 h. The solution was concentrated under reduced pressure. The crude product was washed with ether (200 mL) and ethyl acetate (200 mL) to produce Compound **11** (9.7 g, 96% over two steps)

Compound **11** (5.0 g, 14.15 mmol) and Compound **6** (5.96 g, 1 eq, 14.15 mmol) were dissolved in DMF (50 m) under N_2 gas. HATU (1-[Bis(dimethylamino)methylene]-1H-1,2,3-triazolo[4,5-b]pyridinium 3-Oxide Hexafluorophosphate) (6.99 g,18.40 mmol) and DIPEA (9.86 mL, 56.59 mmol) were added. The reaction mixture was stirred at room temperature for 5 h. The solution was diluted with ethyl acetate and washed with water (x 2), saturated ammonium chloride, saturated sodium bicarbonate, and brine; dried over magnesium sulfate; and concentrated under a rotary evaporator. The crude produce was purified by a silica gel column (40% EtOAC in Hex) to produce Compound **12** (7.4 g, 72%).

To a solution of Compound **12** (7.0 g, 1.38 mmol) in THF:AcOH (70 mL:3.5mL) was added 10% palladium on carbon (0.05 eq). The reaction solution was degassed and charged with hydrogen gas several times. The reaction mixture was stirred at room temperature for overnight. The solution was filtered through Celite pad and concentrated. The crude product was purified by Prep-HPLC (70% ACN in H_2O with 0.035% TFA) to produce "THPA" (3.7 g, 60%) (Figure 2).
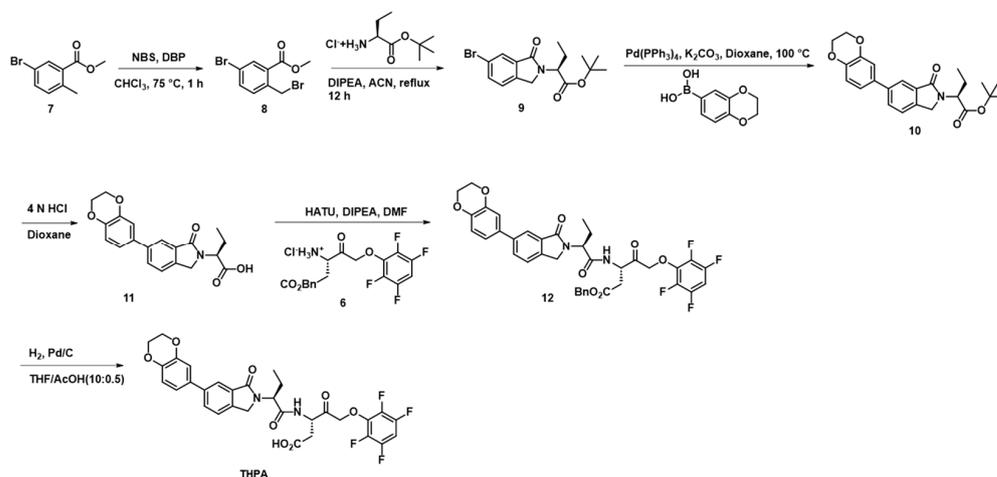

Figure 2. Synthetic scheme of THPA.

1H NMR (400 MHz, DMSO-d6) δ12.51 (s, 1 H), 8.85 (dd, J = 11.2, 7.5 Hz, 1H), 7.91–7.82 (m, 2 H), 7.68 (d, J = 7.8 Hz, 1 H), 7.66–7.52 (m, 1 H), 7.23 (d, J = 8.0 Hz, 2 H), 7.00 (d, J = 8.2 Hz, 1 H), 5.27 (d, J = 4.1 Hz, 2 H), 4.81 (dd, J = 9.7, 5.7 Hz, 1 H), 4.74–4.62 (m, 2 H), 4.53 (d, J = 17.7 Hz, 1 H), 4.33 (s, 4 H), 4.07 (q, J = 7.1 Hz, 1 H), 2.80 (dd, J = 16.9, 6.0 Hz, 1 H), 2.62 (dd, J = 16.9, 7.0 Hz, 1 H), 2.03 (s, 2 H), 1.84 (dq, J = 9.5, 7.2 Hz, 1 H), 1.21 (t, J = 7.1 Hz, 1 H), 0.88 (t, J = 7.3 Hz, 3 H). MS (ESI, LR) Calculated for $C_{31}H_{27}H_4N_2O_8$ (MH+): 631.17, found: 631.2.

2.2. Cell Culture

Human dermal papilla cells (hDPCs) were purchased from Promocell (Promocell, Heidelberg, Germany). Cells were cultured using the growth medium kit in a humidified incubator at 37 °C under 5% CO_2 according to the instructions provided by Promocell. All experiments used cells between passage three and five. Before treatment with THPA and H_2O_2 (Sigma-Aldrich, St. Louis, MO, USA), the medium was replaced with fresh DMEM (WelGENE, Daegu, Republic of Korea) containing 1% FBS (WelGENE, Daegu, Republic of Korea), and cells were incubated for 24 h to reduce the influence of serum and growth factors. Subsequently, THPA and H_2O_2 were treated according to the experimental conditions.

2.3. Cell Viability

Relative cell viability was examined using the WST assay (Daeil Lab Service, Seoul, Republic of Korea) following the manufacturer's protocol. Briefly, hDPCs (5×10^3/well) were seeded into 96-well plates and cultured for 24 h. The medium was replaced with DMEM supplemented with 1% FBS, and the cells were pre-treated with THPA for 4 h. Following H_2O_2 treatment for 24 h, the culture medium was replaced with fresh DMEM media containing 10% WST regent. Absorbance was detected using a microplate reader (Tecan, Mannedorf, Switzerland) at 450 nm.

2.4. Lactate Dehydrogenase Assay

Cytotoxicity was assessed using a Cytotoxicity LDH Assay kit (Dojindo Molecular Technologies, Kumamoto, Japan) following the manufacture's protocol. hDPCs (5×10^3/well) were plated in 96-well plates and incubated for 24 h. hDPCs were pre-treated with THPA for 4 h and exposed to H_2O_2 for 24 h. Following the treatment, the medium was replaced with the working solution. After 30 min, a stop solution was added. The absorbance of the solution in each well was determined using a microplate reader at 490 nm.

2.5. Cellular ROS Detection Assay

The detection of ROS production was performed using the 2′,7′-dichlorofluorescein diacetate (DCFDA)-Cellular ROS Detection Assay kit (Abcam, Cambridge, UK). According to the manufacturer's instructions, hDPCs (5×10^3/well) were seeded into a 96-well microplate. After overnight incubation, the media were removed and cells were washed with buffer. Subsequently, cells were incubated with 25 μM DCFDA at 37 °C for 45 min. After removing DCFDA, supplemented buffer containing THPA and H_2O_2 was added. Fluorescence intensity was measured using a microplate reader at Ex/Em = 485/535 nm.

2.6. TUNEL Staining

Apoptosis was determined using the Click-iT™ plus terminal deoxynucleotidyl transferase dUTP nick end labeling (TUNEL) assay kits for in situ apoptosis detection (Invitrogen) according to the manufacturer's instructions. In brief, hDPCs (3×10^4/well) were seeded in a 24-well plate. Following treatment with THPA and H_2O_2, cells were fixed with 4% paraformaldehyde, permeabilized with a Triton X-100, and incubated with a TdT reaction mixture at 37 °C for 1 h. Counterstaining was performed using DAPI, followed by analysis with fluorescence microscopy (Nikon, Tokyo, Japan).

2.7. Wnt Reporter Assay

WRHEK293A cells were purchased form Amsbio (Amsbio, Abingdon, UK). Cells were seeded in white 96-well plates and incubated overnight. After treatment with H_2O_2 and THPA, cells were lysed using 50 µL of lysis buffer (Thermo Scientific, Waltham, MA, USA). GFP fluorescence was measured using a microplate reader at Ex/Em = 488/510 nm. Subsequently, 50 µL of luciferase substrate solution (Promega, Madison, WI, USA) was added to each well, and luciferase activity was measured. The measured values were normalized using GFP fluorescence.

2.8. Real Time Quantitative Polymerase Chain Reaction

Total RNA was extracted using RNAiso Plus (Takara, Shiaga, Japan). Subsequently, cDNA synthesis was achieved using RevertAid Reverse Transcriptase (Thermo Scientific). Quantitative polymerase chain reaction (qPCR) analysis was conducted utilizing the CFX96 Touch Real-Time PCR Detection System (Bio-Rad, Hercules, CA, USA) and FastStart Essential DNA Probes Master (Roche, Basel, Switzerland), following standard protocols.

2.9. Western Blot

After washing the cells in DPBS, protein was extracted using RIPA lysis solution supplemented with 1 mM PMSF and a protease inhibitor cocktail (Sigma-Aldrich, Missouri, USA). Extracted proteins were equally separated on NuPAGE™ 12% Bis-Tris Gel (Invitrogen, Carlsbad, CA, USA) and transferred onto a PVDF membrane. Following overnight incubation with the appropriate antibodies (Cell Signaling Technology, Danvers, MA, USA) in TBS-T, the membranes were blocked with 5% BSA and subsequently probed with a horseradish peroxidase-conjugated anti-mouse secondary antibody (Bio-Rad).

2.10. Statistical Analysis

Significant F-value items in an ANOVA were evaluated for significance at the $p < 0.05$ level using the Tukey test, which was conducted using SPSS software as the statistical analysis tool.

3. Results

### 3.1. H_2O_2 Induced Cell Death in Cultured hDPCs

H_2O_2 induces hair loss through its cytotoxic effects and the ability to induce oxidative stress [28]. In this study, H_2O_2 was used to induce oxidative stress in hDPCs. To evaluate the cytotoxicity of H_2O_2 on hDPCs, cells were treated with 125 µM–1.5 mM of H_2O_2. The viability of hDPCs was measured using the WST assay after 24 h of treatment. The viability of the hDPCs decreased by approximately 50% at a 1 mM concentration (Figure 3A). In addition, the LDH assay showed a significant increase starting at a 1 mM H_2O_2 concentration (Figure 3B). Based on these results, 1 mM of H_2O_2 was used in subsequent experiments to induce cell death.
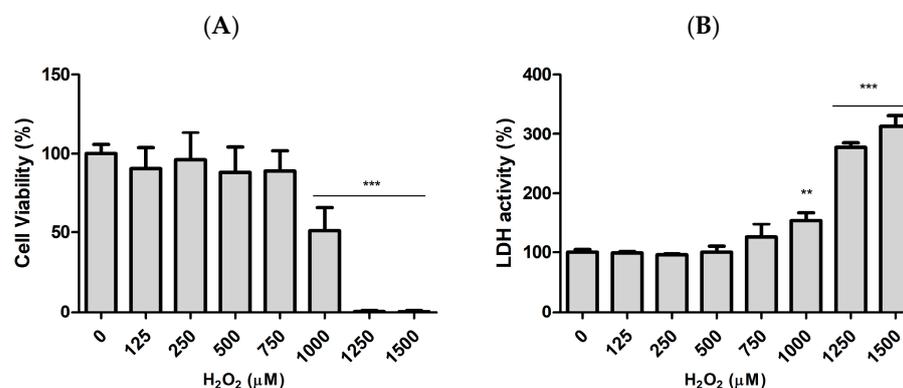
Figure 3. H_2O_2 induces cell apoptosis. Viability (**A**) and LDH (**B**) assays of hDPCs after exposure to different concentrations of H_2O_2 for 24 h, $n = 4$. ** $p < 0.01$, *** $p < 0.001$.

3.2. THPA Protected hDPCs from Cell Apoptosis and Oxidative Damage Induced by H_2O_2

We developed a pan-caspase inhibitor that inhibited all types of caspases, thereby preventing cell apoptosis and oxidative damage induced by H_2O_2. THPA showed no cytotoxicity to the cells at concentrations ranging from 1 nM to 10 uM (Figure S1). THPA was pre-treated with THPA for 4 h prior to H_2O_2 treatment. THPA pre-treatment prevented cell death in hDPCs induced by H_2O_2 in a concentration-dependent manner (Figure 4A). We examined the cellular ROS levels after THPA and H_2O_2 using 2′,7′-dichlorofluorescin diacetate (DCFDA) staining. While 1 mM H_2O_2 significantly increased the cellular ROS level, 5 μM THPA reduced ROS levels (Figure 4B). Furthermore, we performed a TUNEL assay to investigate the inhibitory effect of THPA on the apoptosis of hDPCs. There was a significant increase in the number of TUNEL-positive cells, whereas THPA-treated hDPCs exhibited a reduction in the number of TUNEL-positive cells (Figure 4C).
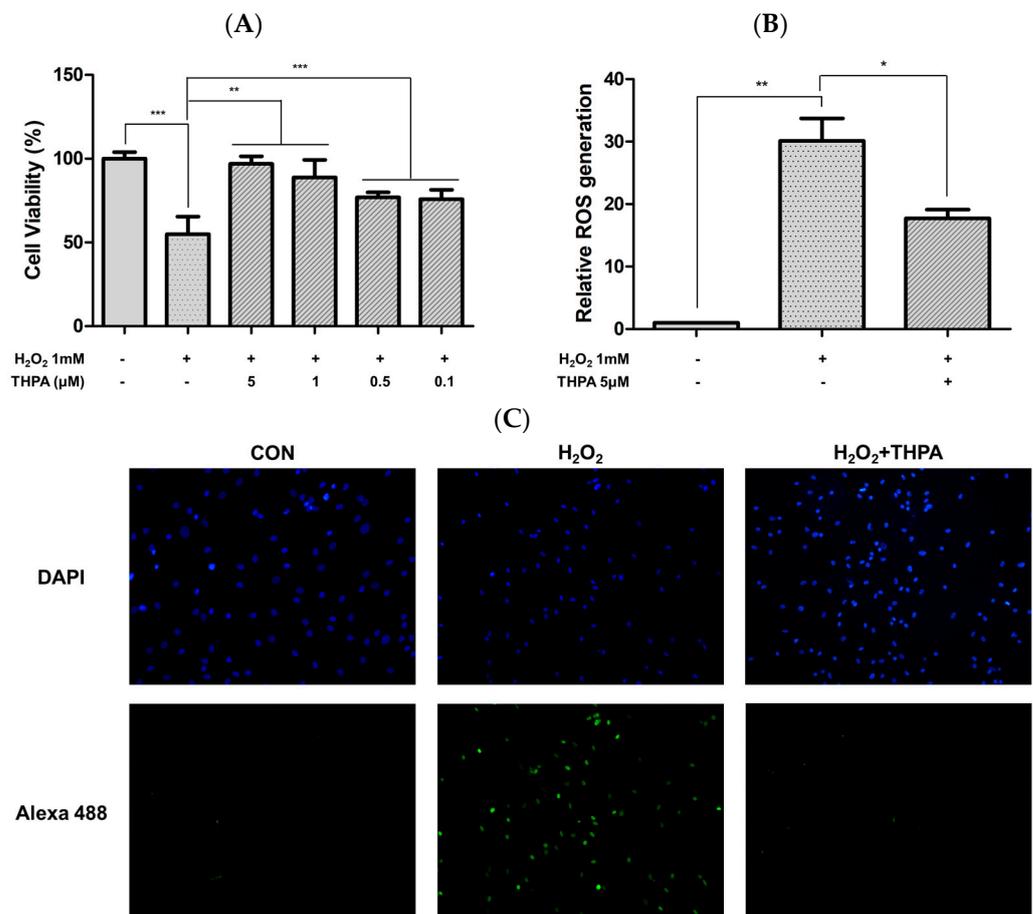

Figure 4. THPA reduced H_2O_2-induced cell apoptosis and oxidative damage. THPA alleviated H_2O_2 effects on hDPCs viability (**A**), ROS level (**B**), apoptosis (**C**), $n = 4$. * $p < 0.05$, **$p < 0.01$, *** $p < 0.001$.

3.3. THPA Inhibited Caspase Activation Induced by H_2O_2

Caspase-3 and caspase-7, which lead to cell apoptosis, are regarded as catagen markers. During catagen, these proteins are highly expressed in the hair matrix and participate in cell fragmentation. Additionally, they mediate the effector mechanisms of apoptosis in human hair follicles [29,30]. PARP is known to respond to DNA damage by activating DNA repair mechanisms and aiding in cell survival. However, when cellular damage is severe or repair is not feasible, PARP promotes cell apoptosis [31]. We investigated the inhibition of apoptosis by measuring the protein expression levels of caspase-3, caspase-7, and PARP following THPA treatment (Figure 5A). Similar to the Western blotting results, THPA significantly blocked the H_2O_2-induced increase in caspase-3/7 activity (Figure 5B).

These results indicated that THPA could prevent catagen entry and cellular damage by preventing apoptosis in hDPCs.
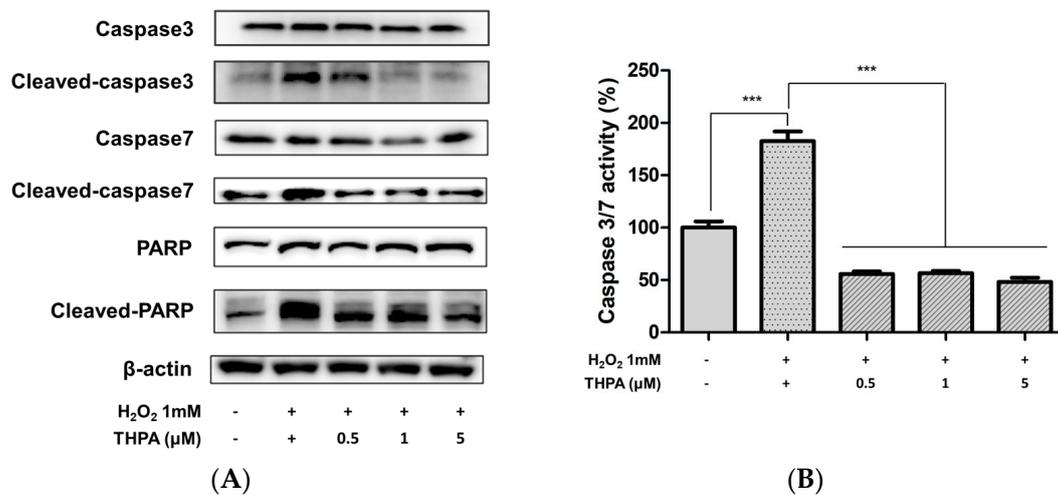
Figure 5. THPA inhibited H_2O_2-induced caspase activity. THPA inhibited H_2O_2-induced caspase activity in hDPCs (**A**,**B**), $n = 3$. *** $p < 0.001$.

3.4. THPA Restored the Reduced β-Catenin Level

The Wnt/β-catenin pathway plays a crucial role in the hair regeneration process [32]. Studies have shown that the inhibition of β-catenin hinders the hair growth cycle, whereas its activation in hDPCs promotes hair growth and prolongs the anagen phase [33–35]. To investigate the effects of H_2O_2 and THPA treatment on Wnt/β-catenin signaling, we examined the protein expression of β-catenin. As shown in Figure 6A, H_2O_2 reduced the protein expressions of β-catenin. This indicated that H_2O_2 treatment affected hair growth and cycling. However, this decrease induced by H_2O_2 was prevented by THPA pre-treatment. Also, a stable Wnt reporter cell line was used to investigate the preventive effects of THPA on the Wnt/β-catenin pathway. Treatment with H_2O_2 decreased Tcf/Lef-mediated reporter activity. However, THPA increased luciferase activity (Figure 6B). This result indicated that THPA stimulates hair regeneration and growth by preventing the decrease in β-catenin levels induced by H_2O_2.
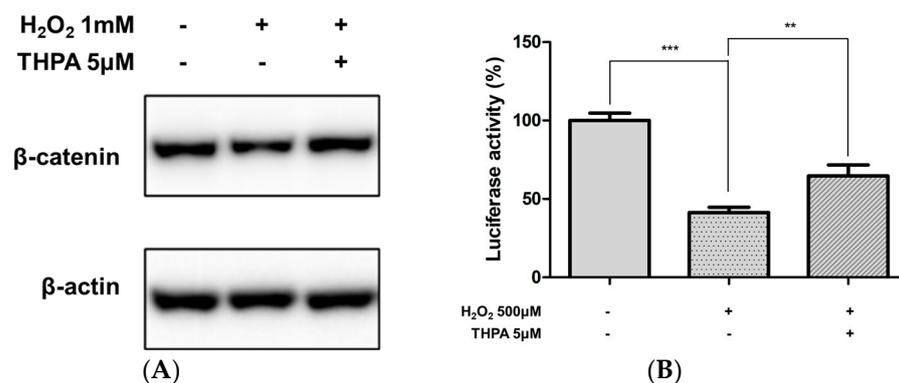

Figure 6. THPA restored the reduced Wnt/β-catenin level. THPA modulates the β-catenin protein expression in hDPCs (**A**) and the activity of Tcf/Lef transcription factor in WRHEK293A cell line (**B**), $n = 3$. ** $p < 0.01$, ***$p < 0.001$.

3.5. Akt/mTOR/p70S6K Signaling Pathway Is Required for Mediating the Effects of THPA on the Inhibition of H_2O_2-Induced Apoptosis

To elucidate the molecular mechanism of action of THPA, we investigated the MAP kinase molecules, which are crucial for cellular signaling cascades. MAP kinases phospho-

rylation was analyzed using a dot blot assay. The phosphorylation of Akt, mTOR, and p70S6K showed the most significant changes (Figure S2). There are studies showing that excessive oxidative stress activates Akt signaling in various cell lines [36–38]. Oxidative stress triggers cell death by inducing Akt activation [39]. Therefore, we further confirmed the changes in the phosphorylation of Akt, mTOR, and p70S6K in response to H_2O_2 and THPA treatment using Western blot. We found that H_2O_2 significantly increased the phosphorylation of Akt, mTOR, and p70S6K, whereas THPA restored their phosphorylation levels (Figure 7A,B).
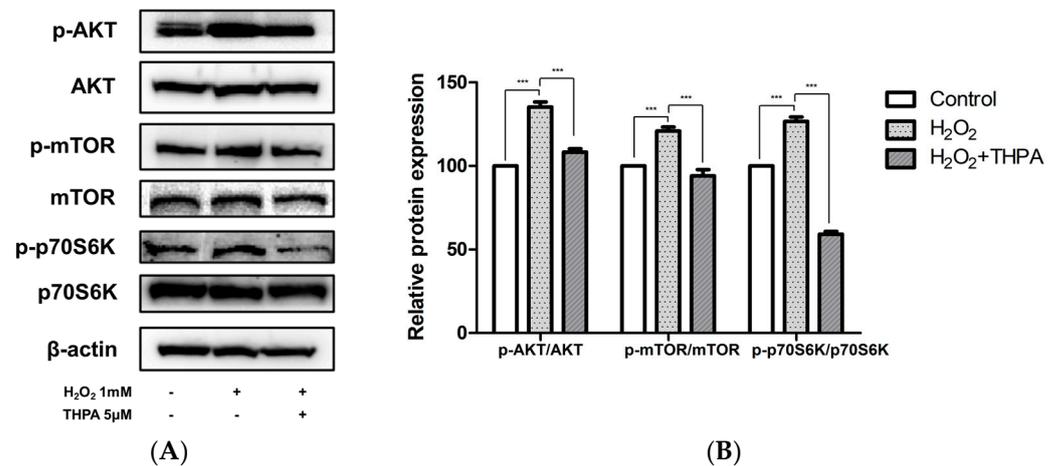
Figure 7. Akt/mTOR/p70S6K signaling is required for mediating the effects of THPA on the inhibition of H_2O_2-induced apoptosis. Protein expression levels of p-AKT, p-mTOR and p-p70S6K were detected by Western blot analysis in hDPCs (**A**,**B**), *n* = 3. *** *p* < 0.001.

3.6. THPA Reduced Catagen and Senescence Markers in H_2O_2-Treated hDPCs

To determine whether THPA prevents catagen and cell senescence induced by H_2O_2, the mRNA expression of the catagen marker DKK-1 and the protein levels of cell senescence markers p16 and p21 were measured. Dickkopf-1 (DKK-1), recognized as a Wnt antagonist and an inducer of catagen, facilitates the regression of hair follicles by inhibiting Wnt/β-catenin signaling [40]. THPA significantly decreased the elevated mRNA level of DKK-1 induced by hydrogen peroxide (Figure 8A). Protein expressions of p21 and p16 were significantly reduced in 5μM of THPA treatment, indicating that cell senescence could be prevented by THPA (Figure 8B).
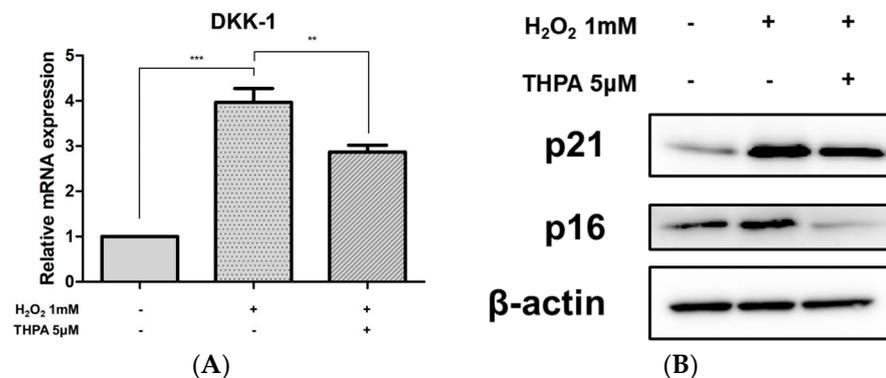
Figure 8. THPA reduced catagen and senescence markers in H_2O_2-treated hDPCs. The mRNA expression of DKK-1 (**A**) and the protein expression of p21 and p16 (**B**) were reduced in H_2O_2-treated hDPCs by THPA. ** *p* < 0.01, *** *p* < 0.001.

4. Discussion

In the present study, we provided in vitro evidence that a pan-caspase inhibitor compound (THPA) can support hair regeneration by preventing of ROS-induced cell damage in hDPCs.

Caspases are a family of genes that are important for maintaining homeostasis by regulating cell death and inflammation, and their inhibition contributes to the prevention of cell death [41]. We found that apoptosis was induced by H_2O_2 and confirmed that THPA prevented it in hDPCs by regulating caspase signaling, which was activated by oxidative stress. Furthermore, the effects of THPA are related to its anti-oxidative effect. The up-regulation of intracellular ROS levels mediated by H_2O_2 was dramatically inhibited following THPA pre-treatment. Recent reports have demonstrated H_2O_2 was reported to induce premature senescence in rat dermal papilla cells, resulting in the inhibition of cell proliferation in follicular keratinocytes [42], and induce cell senescence by cell cycle arrest in hDPCs [43]. These findings suggest that THPA is a novel and potent therapeutic agent against oxidative stress-induced cell dysfunction in hDPCs.

The activation of the Wnt/β-catenin pathway is crucial for the regeneration of hair follicles and the growth of hair shafts. Studies have shown that hair follicles fail to develop when β-catenin, a pivotal signaling molecule within this pathway, undergoes mutation in the hair substrate of mice. Introducing this mutation into normal mice prevented hair follicles from transitioning into the subsequent hair growth cycle. [33] Furthermore, diminished β-catenin activity directly obstructs the differentiation of hair follicle stem cells (HFSCs) from hair follicle cells. [44,45]. As expected, the Wnt/β-catenin pathway was negatively affected by high levels of H_2O_2 in cultured hDPCs. We have found that the decreased expression of β-catenin in cultured hDPCs was restored by THPA.

We conducted a MAPK array to further demonstrate the role of THPA in molecular mechanisms and confirmed significant changes in Akt signaling. It has been reported that Akt activation and downstream signaling involve many pathways implicated in several biological functions, including hair proliferation, regeneration, and survival [46,47]. However, as previously mentioned, there are research findings indicating that Akt activation increases in response to oxidative damage induced by H_2O_2 [39,48]. According to research findings, the PI3K/Akt pathway is involved in various apoptotic signaling pathways. It is believed that the activation of the PI3K/Akt pathway during the early stages of cell apoptosis is understandable. As cell apoptosis progresses, cells exhibit preconditioning properties, where they are protected against apoptosis by a transient insult. Additionally, following withdrawal from a transient apoptotic insult, cells demonstrate self-sustained apoptosis, a remodeling process of apoptosis, that contributes to cell survival. During this apoptotic remodeling process, PI3K/Akt signaling can be inhibited through a negative feedback mechanism, thus providing further protection for cell survival [49,50]

In this context, THPA can prevent the apoptosis of hDPCs by ROS-induced Akt/mTOR/p70S6K activation, indicating that the Akt/mTOR/p70S6K signaling cascade may be the potential mechanism for hair loss.

In both murine and human models, DKK-1, a well-known inhibitor of Wnt/β-catenin signaling, induces apoptosis in hair follicle cells and restricts hair follicle enlargement during regeneration, thereby promoting the transition of anagen hair follicles to the catagen phase [50]. Moreover, the expression of DKK-1 in balding-scalp tissues was elevated compared to non-balding-scalp tissues [51]. Therefore, our data suggest that THPA promotes hair growth by potentially inhibiting the entry into the catagen phase through down-regulating the level of DKK-1 protein.

THPA treatment also significantly reduced the protein expression of the cell senescence markers p21 and p16. Cell senescence involves a state of cell cycle arrest, with key the involvement of regulatory proteins like p21CIP/WAF1 and p16 INK4a. These cyclin-dependent kinase inhibitors play critical roles in controlling the G1/S cell cycle checkpoint [52,53]. In our study, we observed that exposure to H_2O_2 resulted in a signifi-

cant increase in the protein expression levels of p21 and p16. Conversely, THPA treatment reduced the H_2O_2-induced expression of both p21 and p16.

5. Conclusions

Our research offers insights into the cellular and molecular mechanisms by which the caspase inhibitor THPA may protect hair survival in cultured hDPCs. To date, a hair loss treatment utilizing a caspase inhibitor has not been commercialized. Taken together, our data demonstrate that THPA could be a new treatment by preventing cell senescence and premature catagen entry by protecting hDPCs against oxidative stress. Therefore, we propose that THPA should be further investigated in animal and clinical trials to substantiate its potential for preventing hair loss by elucidating its underlying mechanisms.

Abbreviations

hDPCs	human dermal papilla cells
HF	hair follicle
DHT	dihydrotestosterone
THPA	(S)-3-((S)-2-(6-(2,3-dihydrobenzo[b][1,4]dioxin-6-yl)-1-oxoisoindolin-2-yl)butanamido)-4-oxo-5-(2,3,5,6 tetrafluorophenoxy) pentanoic acid
DKK-1	dickkopf-1
ROS	reactive oxidative species
Lef/Tcf	lymphoid enhancer factor/T-cell factor
DCFDA	2′,7′-dichlorofluorescein diacetate
Ex/Em	Excitation/Emission
qPCR	quantitative polymerase chain reaction
TUNEL	terminal deoxynucleotidyl transferase dUTP nick end labeling

References

1. Bruce, A.J.; Pincelli, T.P.; Heckman, M.G.; Desmond, C.M.; Arthurs, J.R.; Diehl, N.N.; Douglass, E.J.; Bruce, C.J.; Shapiro, S.A. A Randomized, Controlled Pilot Trial Comparing Platelet-Rich Plasma to Topical Minoxidil Foam for Treatment of Androgenic Alopecia in Women. *Dermatol. Surg.* **2020**, *46*, 826–832. [CrossRef] [PubMed]

2.   Gasmi, A.; Mujawdiya, P.K.; Beley, N.; Shanaida, M.; Lysiuk, R.; Lenchyk, L.; Noor, S.; Muhammad, A.; Strus, O.; Piscopo, S.; et al. Natural Compounds Used for Treating Hair Loss. *Curr. Pharm. Des.* **2023**, *29*, 1231–1244. [CrossRef] [PubMed]

3.   Malhotra, K.; Madke, B. An updated review on current treatment of alopecia areata and newer therapeutic options. *Int. J. Trichology* **2023**, *15*, 3–12. [CrossRef] [PubMed]

4.   Kost, Y.; Muskat, A.; Mhaimeed, N.; Nazarian, R.S.; Kobets, K. Exosome therapy in hair regeneration: A literature review of the evidence, challenges, and future opportunities. *J. Cosmet. Dermatol.* **2022**, *21*, 3226–3231. [CrossRef] [PubMed]

5.   Sánchez-Díaz, M.; López-Delgado, D.; Montero-Vílchez, T.; Salvador-Rodríguez, L.; Molina-Leyva, A.; Tercedor-Sánchez, J.; Arias-Santiago, S. Systemic Minoxidil Accidental Exposure in a Paediatric Population: A Case Series Study of Cutaneous and Systemic Side Effects. *J. Clin. Med.* **2021**, *10*, 4257. [CrossRef] [PubMed]

6.   Riccio, G.; Sommella, E.; Badolati, N.; Salviati, E.; Bottone, S.; Campiglia, P.; Dentice, M.; Tenore, G.C.; Stornaiuolo, M.; Novellino, E. Annurca apple polyphenols protect murine hair follicles from taxane induced dystrophy and hijacks polyunsaturated fatty acid metabolism toward β-oxidation. *Nutrients* **2018**, *10*, 1808. [CrossRef] [PubMed]

7.   Veraitch, O.; Mabuchi, Y.; Matsuzaki, Y.; Sasaki, T.; Okuno, H.; Tsukashima, A.; Amagai, M.; Okano, H.; Ohyama, M. Induction of hair follicle dermal papilla cell properties in human induced pluripotent stem cell-derived multipotent LNGFR(+)THY-1(+) mesenchymal cells. *Sci. Rep.* **2017**, *7*, 42777. [CrossRef] [PubMed]

8.   Lavker, R.M.; Sun, T.T.; Oshima, H.; Barrandon, Y.; Akiyama, M.; Ferraris, C.; Chevalier, G.; Favier, B.; Jahoda, C.A.; Dhouailly, D.; et al. Hair follicle stem cells. *J. Investig. Dermatol. Symp. Proc.* **2003**, *8*, 28–38. [CrossRef] [PubMed]

9.   Stenn, K.S.; Paus, R. Controls of hair follicle cycling. *Physiol. Rev.* **2001**, *81*, 449–494. [CrossRef]

10. Yano, K.; Brown, L.F.; Detmar, M. Control of hair growth and follicle size by VEGF-mediated angiogenesis. *J. Clin. Investig.* **2001**, *107*, 409–417. [CrossRef]

11. Driskell, R.R.; Clavel, C.; Rendl, M.; Watt, F.M. Hair follicle dermal papilla cells at a glance. *J. Cell Sci.* **2011**, *124*, 1179–1182. [CrossRef] [PubMed]

12. Trüeb, R.M. Oxidative stress in ageing of hair. *Int. J. Trichology* **2009**, *1*, 6–14. [CrossRef] [PubMed]

13. Bichsel, K.J.; Gogia, N.; Malouff, T.; Pena, Z.; Forney, E.; Hammiller, B.; Watson, P.; Hansen, L.A. Role for the epidermal growth factor receptor in chemotherapy-induced alopecia. *PLoS ONE* **2013**, *8*, e69368. [CrossRef] [PubMed]

14. Chen, P.H.; Wang, C.Y.; Hsia, C.W.; Ho, M.Y.; Chen, A.; Tseng, M.J.; Wu, Y.F.; Chen, H.M.; Huang, T.H.; Liu, H.T.; et al. Impact of taxol on dermal papilla cells—A proteomics and bioinformatics analysis. *J. Proteom.* **2011**, *74*, 2760–2773. [CrossRef] [PubMed]

15. Bahta, A.W.; Farjo, N.; Farjo, B.; Philpott, M.P. Premature senescence of balding dermal papilla cells in vitro is associated with p16(INK4a) expression. *J. Investig. Dermatol.* **2008**, *128*, 1088–1094. [CrossRef] [PubMed]

16. Prieto, V.G.; Sadick, N.S.; Shea, C.R. Androgenetic alopecia: Analysis of proliferation and apoptosis. *Arch. Dermatol.* **2002**, *138*, 1101–1102. [CrossRef] [PubMed]

17. Bakry, O.A.; Elshazly, R.M.; Shoeib, M.A.; Gooda, A. Oxidative stress in alopecia areata: A case-control study. *Am. J. Clin. Dermatol.* **2014**, *15*, 57–64. [CrossRef] [PubMed]

18. Shin, H.; Yoo, H.G.; Inui, S.; Itami, S.; Kim, I.G.; Cho, A.R.; Lee, D.H.; Park, W.S.; Kwon, O.; Cho, K.H.; et al. Induction of transforming growth factor-beta 1 by androgen is mediated by reactive oxygen species in hair follicle dermal papilla cells. *BMB Rep.* **2013**, *46*, 460–464. [CrossRef]

19. Elias, P.M.; Schmuth, M. Abnormal skin barrier in the etiopathogenesis of atopic dermatitis. *Curr. Opin. Allergy Clin. Immunol.* **2009**, *9*, 437–446. [CrossRef]

20. Rabbani, P.; Takeo, M.; Chou, W.; Myung, P.; Bosenberg, M.; Chin, L.; Taketo, M.M.; Ito, M. Coordinated activation of Wnt in epithelial and melanocyte stem cells initiates pigmented hair regeneration. *Cell* **2011**, *145*, 941–955. [CrossRef]

21. Myung, P.S.; Takeo, M.; Ito, M.; Atit, R.P. Epithelial Wnt ligand secretion is required for adult hair follicle growth and regeneration. *J. Investig. Dermatol.* **2013**, *133*, 31–41. [CrossRef]

22. Liu, B.; Chen, X.; Yi, H.; Han, L.; Ji, B.; Chen, H.; Deng, W.; Wan, M. β-Catenin is involved in oleanolic acid-dependent promotion of proliferation in human hair matrix cells in an in vitro organ culture model. *Fitoterapia* **2017**, *121*, 136–140. [CrossRef]

23. Jahoda, C.A.B.; Reynolds, A.J. Dermal-epidermal interactions-follicle-derived cell populations in the study of hair-growth mechanisms. *J. Investig. Dermatol.* **1993**, *101*, 33–38. [CrossRef]

24. Ohn, J.; Kim, S.J.; Choi, S.J.; Choe, Y.S.; Kwon, O.; Kim, K.H. Hydrogen peroxide (H_2O_2) suppresses hair growth through downregulation of β-catenin. *J. Dermatol. Sci.* **2018**, *89*, 91–94. [CrossRef] [PubMed]

25. Deng, W.; Wang, Y.; Long, X.; Zhao, R.; Wang, Z.; Liu, Z.; Cao, S.; Shi, B. miR-21 Reduces Hydrogen Peroxide-Induced Apoptosis in c-kit+ Cardiac Stem Cells In Vitro through PTEN/PI3K/Akt Signaling. *Oxidative Med. Cell. Longev.* **2016**, *2016*, 5389181. [CrossRef] [PubMed]

26. Nirmaladevi, D.; Venkataramana, M.; Chandranayaka, S.; Ramesha, A.; Jameel, N.M.; Srinivas, C. Neuroprotective effects of bikaverin on H_2O_2-induced oxidative stress mediated neuronal damage in SH-SY5Y cell line. *Cell Mol. Neurobiol.* **2014**, *34*, 973–985. [CrossRef] [PubMed]

27. Thianthanyakij, T.; Zhou, Y.; Wu, M.; Zhang, Y.; Lin, J.M.; Huang, Y.; Sha, Y.; Wang, J.; Kong, S.P.; Lin, J.; et al. Salvianolic Acid B Reduces Oxidative Stress to Promote Hair-Growth in Mice, Human Hair Follicles and Dermal Papilla Cells. *Clin. Cosmet. Investig. Dermatol.* **2024**, *17*, 791–804. [CrossRef]

28. Seo, J.A.; Bae, I.H.; Jang, W.H.; Kim, J.H.; Bak, S.Y.; Han, S.H.; Park, Y.H.; Lim, K.M. Hydrogen peroxide and monoethanolamine are the key causative ingredients for hair dye-induced dermatitis and hair loss. *J. Dermatol. Sci.* **2012**, *66*, 12–19. [CrossRef]

29. Lindner, G.; Botchkarev, V.A.; Botchkareva, N.V.; Ling, G.; van der Veen, C.; Paus, R. Analysis of apoptosis during hair follicle regression (catagen). *Am. J. Pathol.* **1997**, *151*, 1601–1617.

30. Soma, T.; Ogo, M.; Suzuki, J.; Takahashi, T.; Hibino, T. Analysis of apoptotic cell death in human hair follicles in vivo and in vitro. *J. Investig. Dermatol.* **1998**, *111*, 948–954. [CrossRef]

31. Bouchard, V.J.; Rouleau, M.; Poirier, G.G. PARP-1, a determinant of cell survival in response to DNA damage. *Exp. Hematol.* **2003**, *31*, 446–454. [CrossRef] [PubMed]

32. Houschyar, K.S.; Momeni, A.; Pyles, M.N.; Maan, Z.N.; Whittam, A.J.; Siemers, F. Wnt signaling induces epithelial differentiation during cutaneous wound healing. *Organogenesis* **2015**, *11*, 95–104. [CrossRef] [PubMed]

33. Huelsken, J.; Vogel, R.; Erdmann, B.; Cotsarelis, G.; Birchmeier, W. beta-Catenin controls hair follicle morphogenesis and stem cell differentiation in the skin. *Cell* **2001**, *105*, 533–545. [CrossRef]

34. Ouji, Y.; Yoshikawa, M.; Moriya, K.; Nishiofuku, M.; Matsuda, R.; Ishizaka, S. Wnt-10b, uniquely among Wnts, promotes epithelial differentiation and shaft growth. *Biochem. Biophys. Res. Commun.* **2008**, *367*, 299–304. [CrossRef] [PubMed]

35. Zhou, L.; Xu, M.; Yang, Y.; Yang, K.; Wickett, R.R.; Andl, T.; Millar, S.E.; Zhang, Y. Activation of β-Catenin Signaling in CD133-Positive Dermal Papilla Cells Drives Postnatal Hair Growth. *PLoS ONE* **2016**, *11*, e0160425. [CrossRef] [PubMed]

36. Yuan, T.L.; Cantley, L.C. PI3K pathway alterations in cancer: Variations on a theme. *Oncogene* **2008**, *27*, 5497–5510. [CrossRef] [PubMed]

37. Kaushal, G.P.; Liu, L.; Kaushal, V.; Hong, X.; Melnyk, O.; Seth, R.; Safirstein, R.; Shah, S.V. Regulation of caspase-3 and -9 activation in oxidant stress to RTE by forkhead transcription factors, Bcl-2 proteins, and MAP kinases. *Am. J. Physiol. Renal Physiol.* **2004**, *287*, F1258–F1268. [CrossRef] [PubMed]

38. Mo, L.; Yang, C.; Gu, M.; Zheng, D.; Lin, L.; Wang, X.; Lan, A.; Hu, F.; Feng, J. PI3K/Akt signaling pathway-induced heme oxygenase-1 upregulation mediates the adaptive cytoprotection of hydrogen peroxide preconditioning against oxidative injury in PC12 cells. *Int. J. Mol. Med.* **2012**, *30*, 314–320. [CrossRef]

39. Chetram, M.A.; Bethea, D.A.; Odero-Marah, V.A.; Don-Salu-Hewage, A.S.; Jones, K.J.; Hinton, C.V. ROS-mediated activation of AKT induces apoptosis via pVHL in prostate cancer cells. *Mol. Cell Biochem.* **2013**, *376*, 63–71. [CrossRef]

40. Choi, Y.H.; Shin, J.Y.; Kim, J.; Kang, N.G.; Lee, S. Niacinamide Down-Regulates the Expression of DKK-1 and Protects Cells from Oxidative Stress in Cultured Human Dermal Papilla Cells. *Clin. Cosmet. Investig. Dermatol.* **2021**, *14*, 1519–1528. [CrossRef]

41. McIlwain, D.R.; Berger, T.; Mak, T.W. Caspase functions in cell death and disease. *Cold Spring Harb. Perspect. Biol.* **2013**, *5*, a008656. [CrossRef] [PubMed]

42. Huang, W.Y.; Huang, Y.C.; Huang, K.S.; Chan, C.C.; Chiu, H.Y.; Tsai, R.Y.; Chan, J.Y.; Lin, S.J. Stress-induced premature senescence of dermal papilla cells compromises hair follicle epithelial-mesenchymal interaction. *J. Dermatol. Sci.* **2017**, *86*, 114–122. [CrossRef]

43. Bae, S.; Lim, K.M.; Cha, H.J.; An, I.S.; Lee, J.P.; Lee, K.S.; Lee, G.T.; Lee, K.K.; Jung, H.J.; Ahn, K.J.; et al. Arctiin blocks hydrogen peroxide-induced senescence and cell death though microRNA expression changes in human dermal papilla cells. *Biol. Res.* **2014**, *47*, 50. [CrossRef]

44. Povelones, M.; Nusse, R. Wnt signalling sees spots. *Nat. Cell Biol.* **2002**, *4*, 249–250. [CrossRef] [PubMed]

45. Furlong, E.E.A. Functional genomics approach to identify new regulators of Wnt signaling. *Dev. Cell* **2005**, *8*, 624–626. [CrossRef] [PubMed]

46. Chen, Y.; Fan, Z.; Wang, X.; Mo, M.; Zeng, S.B.; Xu, R.H.; Wang, X.; Wu, Y. PI3K/Akt signaling pathway is essential for de novo hair follicle regeneration. *Stem. Cell Res. Ther.* **2020**, *11*, 144. [CrossRef]

47. Kang, J.I.; Choi, Y.K.; Koh, Y.S.; Hyun, J.W.; Kang, J.H.; Lee, K.S.; Lee, C.M.; Yoo, E.S.; Kang, H.K. Vanillic Acid Stimulates Anagen Signaling via the PI3K/Akt/β-Catenin Pathway in Dermal Papilla Cells. *Biomol. Ther.* **2020**, *28*, 354–360. [CrossRef]

48. Li, D.; Ni, S.; Miao, K.S.; Zhuang, C. PI3K/Akt and caspase pathways mediate oxidative stress-induced chondrocyte apoptosis. *Cell Stress Chaperones* **2019**, *24*, 195–202. [CrossRef]

49. Facchini, A.; Stanic, I.; Cetrullo, S.; Borzì, R.M.; Filardo, G.; Flamigni, F. Sulforaphane protects human chondrocytes against cell death induced by various stimuli. *J. Cell Physiol.* **2011**, *226*, 1771–1779. [CrossRef]

50. Lei, M.; Guo, H.; Qiu, W.; Lai, X.; Yang, T.; Widelitz, R.B.; Chuong, C.M.; Lian, X.; Yang, L. Modulating hair follicle size with Wnt10b/DKK1 during hair regeneration. *Exp. Dermatol.* **2014**, *23*, 407–413. [CrossRef]

51. Shinomura, T.; Nishida, Y.; Ito, K.; Kimata, K. cDNA cloning of PG-M, a large chondroitin sulfate proteoglycan expressed during chondrogenesis in chick limb buds. Alternative spliced multiforms of PG-M and their relationships to versican. *J. Biol. Chem.* **1993**, *268*, 14461–14469. [CrossRef] [PubMed]

52. Waga, S.; Hannon, G.J.; Beach, D.; Stillman, B. The p21 inhibitor of cyclin-dependent kinases controls DNA replication by interaction with PCNA. *Nature* **1994**, *369*, 574–578. [CrossRef] [PubMed]

53. Waga, S.; Hannon, G.J.; Beach, D.; Stillman, B. p16INK4A participates in a G1 arrest checkpoint in response to DNA damage. *Mol. Cell Biol.* **1998**, *18*, 378–387.